

High-magnification vascular imaging to reject false-positive sites *in situ* during Hexvix[®] fluorescence cystoscopy

Blaise Lovisa

Ecole Polytechnique Fédérale de Lausanne
Medical Photonics Group
Station 6
CH-1015 Lausanne, Switzerland

Patrice Jichlinski

CHUV University Hospital
Department of Urology
CH-1011 Lausanne, Switzerland

Bernd-Claus Weber

Richard Wolf GmbH
Pforzheimerstrasse 32
D-75438 Knittlingen, Germany

Daniela Aymon

CHUV University Hospital
Department of Urology
CH-1011 Lausanne, Switzerland

Hubert van den Bergh

Georges Wagnières
Ecole Polytechnique Fédérale de Lausanne
Medical Photonics Group
Station 6
CH-1015 Lausanne, Switzerland

1 Introduction

Bladder cancer is the fourth most common cancer among men and the eighth most common malignancy in women in the Western world.¹ Urothelial cell carcinoma comprises 90% to 95% of all bladder cancers, with about 70% found initially as non-muscle-invasive bladder cancer and the remainder as invasive cancer.² Flat lesions, such as high-grade dysplasia or carcinoma *in situ*, are associated with a high risk of invasive progression, and an even higher recurrence rate (50 to 85%).³ Therefore, there is a need for a reliable early detection method.

Over the past decades, white-light (WL) cystoscopy was established as the standard diagnostic procedure to detect early bladder cancer. However, WL may lead to missing lesions that are difficult or impossible to visualize.⁴ To overcome this limitation, fluorescence cystoscopy based on aminolevulinic acid (5-ALA) and its derivatives has now been well established. The fluorescence cystoscopy is performed using blue-violet light that excites the red fluorescence of the

Abstract. Fluorescence imaging for detection of non-muscle-invasive bladder cancer is based on the selective production and accumulation of fluorescing porphyrins—mainly, protoporphyrin IX—in cancerous tissues after the instillation of Hexvix[®]. Although the sensitivity of this procedure is very good, its specificity is somewhat limited due to fluorescence false-positive sites. Consequently, magnification cystoscopy has been investigated in order to discriminate false from true fluorescence positive findings. Both white-light and fluorescence modes are possible with the magnification cystoscope, allowing observation of the bladder wall with magnification ranging between 30× for standard observation and 650×. The optical zooming setup allows adjusting the magnification continuously *in situ*. In the high-magnification (HM) regime, the smallest diameter of the field of view is 600 microns and the resolution is 2.5 microns when in contact with the bladder wall. With this cystoscope, we characterized the superficial vascularization of the fluorescing sites in order to discriminate cancerous from noncancerous tissues. This procedure allowed us to establish a classification based on observed vascular patterns. Seventy-two patients subject to Hexvix[®] fluorescence cystoscopy were included in the study. Comparison of HM cystoscopy classification with histopathology results confirmed 32/33 (97%) cancerous biopsies and rejected 17/20 (85%) noncancerous lesions. © 2010 Society of Photo-Optical Instrumentation Engineers. [DOI: 10.1117/1.3484257]

Keywords: nonmuscle invasive bladder cancer; fluorescence cystoscopy; high magnification; vessel patterns; vasculogenesis; angiogenesis.

Paper 101495SR received Mar. 24, 2010; revised manuscript received May 27, 2010; accepted for publication Jun. 2, 2010; published online Sep. 2, 2010.

porphyrins, mainly protoporphyrin IX (PpIX).^{5,6} In the biosynthesis of heme, endogenous 5-ALA is a natural precursor of the fluorescing PpIX.⁷ The subsequent conversion of PpIX into heme is relatively slow. The application of exogenous ALA-derivatives, including Hexvix[®], can thus lead to accumulation of significant concentrations of fluorescing porphyrins. The latter are selectively produced and accumulated in these early lesions upon the instillation of the bladder with a solution of Hexvix[®] over about one hour.^{8,9} With this method, the sensitivity of cystoscopy for flat lesions that are overlooked in white light is improved to nearly 100%.⁸⁻¹⁰ Thus, fluorescence cystoscopy will reveal areas in the bladder that are suspicious for flat lesions (dysplasia, pTis) or small papillary tumors (pTa, pT1) that can not always easily be seen with WL cystoscopy.^{11,12} Furthermore, it has been shown that fluorescence cystoscopy reduces the tumor recurrence rate, probably due to a more complete resection.¹³⁻¹⁶

Fluorescence cystoscopy has a high sensitivity but still yields a relatively high percentage of fluorescence false-positive lesions—typically, 39%.^{11,12} Histopathological diagnosis of the false-positives showed that false fluorescence

Address all correspondence to: Georges Wagnières, Ecole Polytechnique Fédérale Lausanne (EPFL), ISIC-GE, Station 6, CH-1015, Lausanne, Switzerland. Tel: 41-216-933-120; Fax: 41-216-935-110; E-mail: georges.wagnieres@epfl.ch

mostly occurred in tissues with a high cell turnover such as metaplasia, hyperplasia, and chronic inflammation.⁹

In 2005, the European Association of Urology (EAU) approved fluorescence cystoscopy as the standard method for the detection of non-muscle-invasive bladder cancer.¹⁷ The FDA granted approval for the HAL-based fluorescence photodetection in May 2010. There is clear evidence that the features of angiogenesis (such as microvessel density) and expression of angiogenic factors are related to adverse outcomes in bladder cancer.¹⁸ Reiher et al. confirmed the strong association of microvessel density with the well-established prognostic factors of grade and stage in non-muscle-invasive bladder cancer.¹⁹

It is likely that developing new imaging capabilities for vascular imaging will also facilitate discriminating mucosal changes in the bladder. Vascular patterns, like tortuous vessels and vessel loops, are used to identify neoplasia in several organs, including the bronchi and the upper and lower gastrointestinal tract.^{20–23} In bronchoscopic studies, Shibuya et al. state that conventional white-light bronchoscopes observe only increased redness and local swelling, whereas high-magnification bronchoscopes enable the vascular network to be visualized in the bronchial mucosa.^{22,23} Morphological features such as vessel growth and complex networks of tortuous vessels help these authors to identify this cancerization process.²³ Indeed, they were able to distinguish between inflammatory tissue and neoplastic lesion in the bronchi by observing the complex neovascular structure and tortuosity. Different groups showed that a zooming observation allows us to observe changes in the intrapapillary capillary loops in the esophagus, including dilatation, weaving, changes in caliber, and differences in shape.^{21,24} They also observed that the tumor vessels were rearranged at the surface of the tumor. Similarly, East et al. defined the vascular pattern intensity, which is directly related to the microvessel density, in combination with the Kudo pit pattern classification, to assess the malignancy of small colonic polyps.²⁰

With the development of high-magnification (HM) cystoscopy presented in this manuscript, it is possible to visualize alterations of the vascular organization at the surface of the bladder mucosa. Due to its optical zoom, our cystoscope allows us to adjust the magnification continuously between the low- and high-magnification regimes by turning a knob and changing the distance between the cystoscope tip and the mucosa. As compared to cellular imaging systems, the operator is able to first localize the area of interest with the help of fluorescence cystoscopy, and then to zoom in, to characterize the superficial vascularization, using a single device. Therefore, HM examination fits easily into the clinical routine, as it does not require much extra time and instrumentation.

The present study evaluates this vascular imaging technology on patients who were subject to routine fluorescence cystoscopy. To our knowledge, this is the first time that vascularization patterns are used as a discrimination criterion on fluorescence positive spots in the bladder. A flexible videocystoscope will be designed based on the results of this study in order to allow an observation of the whole bladder in both low- and high-magnification regimes.



Fig. 1 Magnification can be adjusted with a knob on the optical device (range 30 to 650 \times).

2 Materials and Methods

2.1 High-Magnification Setup

The bladder was first inspected with a conventional fluorescence cystoscope to localize the fluorescence positive sites under blue-violet light. The accessible fluorescing sites were then observed with the rigid magnification cystoscope (Lumina Microview 25 deg, Richard Wolf GmbH, Germany). This cystoscope (see Fig. 1) was first operated in a low-magnification regime to identify the fluorescence positive lesions in fluorescence mode, and then in an HM regime to characterize the vascularization under white-light reflectance mode. This approach is quite convenient, since it enables us to observe the bladder wall with magnification ranging continuously between 30 \times and 650 \times under fluorescence or white-light observation, without changing the cystoscope.

The HM cystoscope has an external diameter of 4 mm and is equipped with a knob allowing alteration of the magnification *in situ*. This continuous range is achieved by simultaneously adjusting the device's focal length and the cystoscope–tissue distance. The magnification is defined here as the ratio between the sizes of the object on the image displayed on a 19-in monitor and the corresponding real object, given that our conventional cystoscope yields a 30 \times magnification. The present device is able to resolve patterns down to element 5 of group 7 on the USAF target 1951 (line width: 2.5 μm , corresponding to 200 lp/mm; picture not shown).

2.2 Endoscopic Image Classification

The whole procedure was recorded on a DV recorder (DV-CAM DSR 20MDP, Sony Corporation, Tokyo, Japan) and digitized using the IEEE1394 connection between the DV recorder and a portable PC. In an explorative preliminary study (data not shown), individual frames were extracted from the video sequences, and image classification was performed offline based on visual quantification of the vessel patterns. Images were classified in five categories: (A) linear—i.e., normal—vascularization; (B) edema and/or vessel thickening; (C) tortuous vessels and/or vessel loops; (D) dense mesh and/or disorganized network; and (E) no vascularization visualized while probing the lesion. In the latter, the images were excluded from the statistics. Typical HM images on flat fluorescence positive sites are shown in Fig. 2 according to the classification.

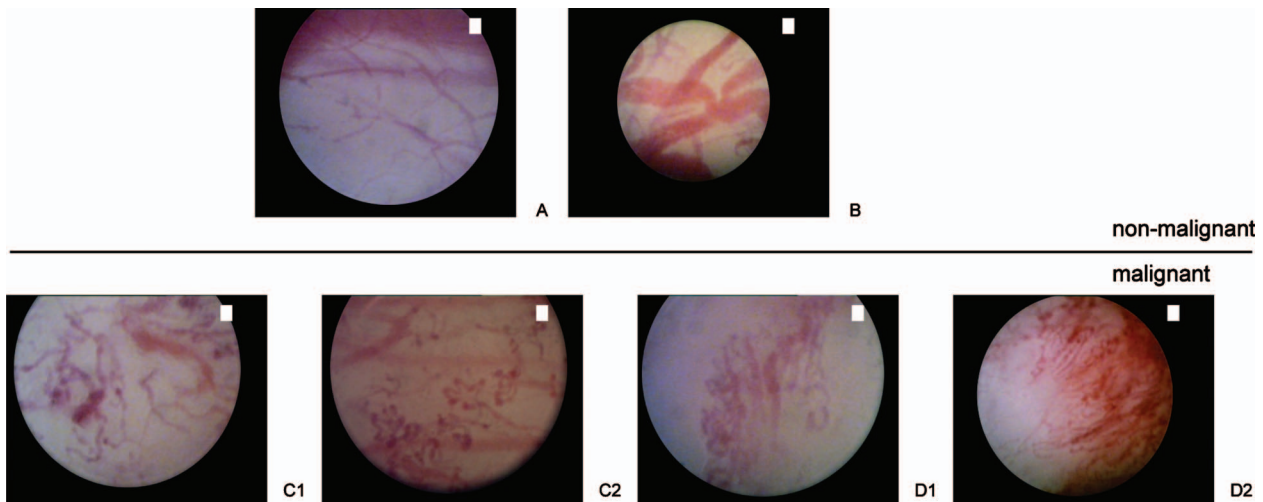


Fig. 2 High-magnification endoscopic images acquired under white light. Nonmalignant: (A) normal vessels, (B) edema and vessel thickening. Malignant: (C1) tortuous vessels, (C2) vessel loops, (D1) dense mesh, (D2) disorganized network.

In the study presented here, the vascularization patterns were classified intraoperatively based on these categories (A to E). DV recording was used only for documentation purposes.

2.3 Patient Population

Seventy-eight patients (54 men, 24 women; mean age 67; range 18 to 85) with suspected or verified bladder cancer (by means of positive urinary cytology, prior cystoscopy, or a history of urothelial cancer) were enrolled between September 2007 and August 2009. They underwent fluorescence cystoscopy with Hexvix[®] at the CHUV University Hospital (Lausanne, Switzerland), under loco-regional or general anesthesia. Patients were informed about the benefits and risks of the fluorescence procedure, and the study was acknowledged by the local ethics committee.

2.4 Endoscopic Procedure

Hexvix[®] (GE Healthcare, Chalfont St. Giles, U.K.) was prepared by reconstitution of 100 mg of hexaminolevulinate (HAL) hydrochloride powder, equivalent to 85 mg of HAL, in 50 ml phosphate buffered saline (PBS). Following hospitalization, patients received an intravesical instillation of 50 ml (8 mM) solution of Hexvix[®] through a standard catheter for about one hour. After emptying of the bladder, inspection and mapping of all lesions and suspicious areas was done by an urologist with experience in this method.

2.5 Imaging System

The endoscopic fluorescence imaging system basically consists of a filtered light source and a filtered endoscopic camera, as shown schematically in Fig. 3. Fluorescence cystoscopy was performed using a commercial system (Richard

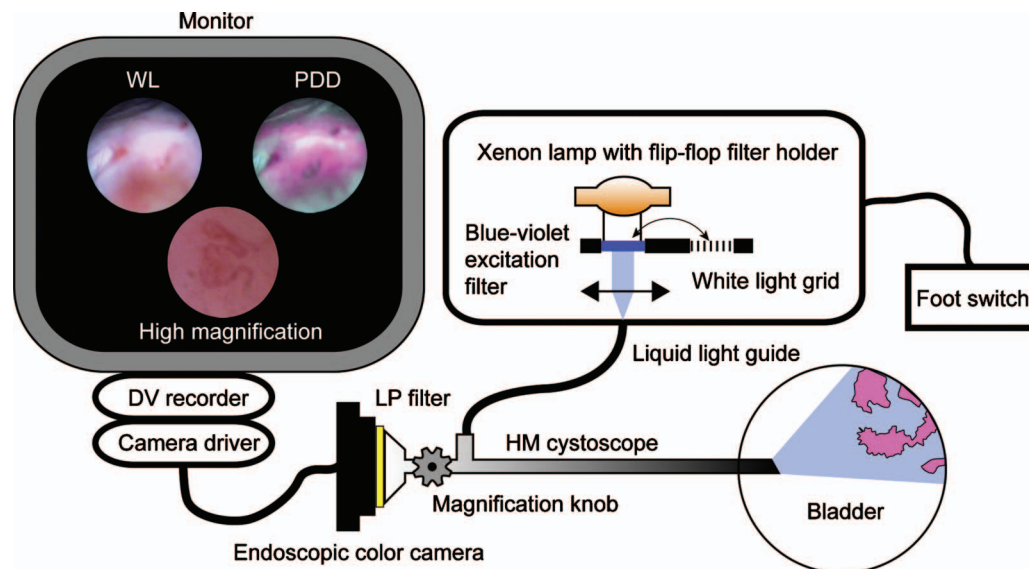


Fig. 3 Fluorescence cystoscopy setup.

Table 1(a) Histopathological analysis of all fluorescence positive (HAL+) lesions ($n=179$).

| | No. detected on HAL+ sites | | | | | |
|---------------------------------------|----------------------------|-------------------|------------|-----------|-------------------|----------|
| | HAL+ | With inflammation | | WL+ | With inflammation | |
| Dysplasia | 18 | 7 | 111 HAL/TP | 8 | 5 | 72 WL/TP |
| pTa (G ₁ -G ₃) | 43 | 3 | | 33 | 1 | |
| pT1 (G ₁ -G ₂) | 12 | 0 | | 11 | 0 | |
| pT2 | 4 | 0 | | 4 | 0 | |
| pTis | 34 | 7 | | 15 | 4 | |
| Nonmalignant | 68 | 41 | 68 HAL/FP | 27 | 17 | 27 WL/FP |
| Total | 179 | 58 | | 99 | 27 | |

Table 1(b) Histopathological analysis of the macroscopically flat fluorescence positive (HAL+) lesions ($n=111$).

| | No. detected on flat HAL+ sites | | | | | |
|---------------------------------------|---------------------------------|-------------------|-----------|-----------|-------------------|----------|
| | HAL+ | With inflammation | | WL+ | With inflammation | |
| Dysplasia | 15 | 5 | 58 HAL/TP | 5 | 3 | 23 WL/TP |
| pTa (G ₁ -G ₃) | 10 | 1 | | 5 | 0 | |
| pT1 (G ₁ -G ₂) | 4 | 0 | | 3 | 0 | |
| pT2 | 0 | 0 | | 0 | 0 | |
| pTis | 29 | 6 | | 10 | 3 | |
| No tumor | 53 | 29 | 53 HAL/FP | 16 | 8 | 16 WL/FP |
| Total | 111 | 41 | | 39 | 14 | |

Wolf GmbH, Knittlingen, Germany), which allowed bladder wall inspection with both white-light reflectance and blue-violet light excited fluorescence. The endoscopic light source is based on an IR filtered 300-W Xenon lamp (Richard Wolf GmbH) equipped with a flip-flop filter holder containing a light-attenuation grid for conventional white-light illumination and a blue-violet interference filter (390 to 440 nm) to excite the fluorescence of the porphyrins—mainly, PpIX. The camera collects the red fluorescence and the tissue autofluorescence through a long-pass filter (cut-on wavelength 450 nm). A foot switch allows rapid changing between white-light illumination and blue-violet fluorescence excitation. The source light is delivered to the cystoscope optics by a liquid light guide.

2.6 Histopathological Analysis

Each fluorescing positive site was cold-biopsied and/or resected. Tissue samples were fixed in formalin and examined by an experienced pathologist who was blinded to the high-magnification description of the vascularization. Urothelial carcinomas were graded according to the World Health Orga-

nization (WHO) 1973 classification²⁵ and to the WHO/International Society of Urological Pathology (ISUP) 1998 consensus.²⁶ Fluorescence positive biopsies were then grouped into two classes: nonmalignant (normal, metaplasia, hyperplasia, and chronic inflammation) and malignant (dysplasia, pTa, pT1, p, and pTis).

3 Results

3.1 Histopathology

A total of 179 biopsies taken on fluorescence positive (HAL+) spots were biopsied. They were macroscopically classified as being 111 flat, 51 exophytic, and 17 scar tissues. In this study, we retained the macroscopic description, i.e., flat versus exophytic, given by the operator intraoperatively, even if it differs from the pathological description. Ten pTa and 4 pT1 appeared flat, whereas 3 pTis and 1 dysplasia appeared exophytic.

The regions of interest that initially tested as fluorescence positive (HAL+) or white-light positive (WL+) but upon pathological analysis were described as noncancerous biop-

Table 2(a) visual classification of all the fluorescence positive lesions ($n=58$) observed with high magnification: 36 true-positive (HAL/TP) and 22 false-positive (HAL/FP).

| HM descriptive analysis | | 36 HAL/TP | | 22 HAL/FP | |
|-------------------------|-------------------------------------|-----------|----------|-----------|----------|
| Nonmalignant | (A) Linear vascularization | 0 | 1 HM/FN | 15 | 17 HM/TN |
| | (B) Edema and vessel thickening | 1 | | 2 | |
| Malignant | (C) Tortuous vessels/vessel loops | 22 | 32 HM/TP | 2 | 3 HM/FP |
| | (D) Dense mesh/disorganized network | 10 | | 1 | |
| Total | | 33 | | 20 | |
| Discarded | (E) No visualized vascularization | 3 | | 2 | |

Table 2(b) visual classification of the macroscopically flat fluorescence positive lesions ($n=45$) observed with high magnification: 24 true-positive (HAL/TP) and 21 false-positive (HAL/FP).

| HM descriptive analysis of the flat lesions | | 24 HAL/TP | | 21 HAL/FP | |
|---|-------------------------------------|-----------|----------|-----------|----------|
| Nonmalignant | (A) Linear vascularization | 0 | 0 HM/FN | 15 | 17 HM/TN |
| | (B) Edema and vessel thickening | 0 | | 2 | |
| Malignant | (C) Tortuous vessels/vessel loops | 12 | 22 HM/TP | 2 | 2 HM/FP |
| | (D) Dense mesh/disorganized network | 10 | | 0 | |
| Total | | 22 | | 19 | |
| Discarded | (E) No visualized vascularization | 2 | | 2 | |

sies were characterized as false-positives (HAL/FP and WL/FP, respectively). Similarly, HAL+ and WL+ regions of interest that demonstrated cancerous biopsies were characterized as true-positives (HAL/TP and EL/TP, respectively).

Table 1(a) shows the histopathological analysis of the 179 HAL+ biopsies, detected by Hexvix[®] and WL cystoscopy, respectively. The additional columns list how many biopsies contained inflammatory tissue. Table 1(b) shows the same data for flat lesions only.

We can observe that fluorescence cystoscopy is much more sensitive to early lesions than WL cystoscopy [see Table 1(a)], even in this case of a very experienced WL endoscopist. Indeed, 39 additional lesions were discovered with the help of Hexvix[®] cystoscopy. Table 1(a) shows that inflammation is present in 41/68 (61%) of the HAL/FP, whereas this is the case in only 17/111 (15%) of the HAL/TP. Table 1(b) shows that the same observation is valid for flat lesions; inflammatory tissue is present in 29/53 (55%) of the HAL/FP, whereas this is the case in only 12/58 (21%) of the HAL/TP. Thirty-five additional flat lesions were discovered with the help of Hexvix[®] cystoscopy. It is interesting to note that no inflammatory tissue was found in the pT1 and p cancers.

3.2 High-Magnification Descriptive Analysis

Among the 179 biopsies, 58 HAL+ sites from which 45 flat lesions were observed with high magnification in order to try to decrease the number of FP, and thus the number of biopsies taken. The HM clinically observed blood vessels were classi-

fied into four categories: (A) normal or linear vascularization; (B) edema and vessel thickening; (C) tortuous vessels/vessel loops; (D) dense mesh/disorganized network. Biopsies that were classified as cancerous and could be attributed with either HM classifications A and B are referred to as HM false-negative (HM/FN), while HM classifications C and D are referred to as HM true-positive (HM/TP). Conversely, biopsies that were classified as noncancerous and could be attributed with either HM classification A and B are referred to as HM true-negative (HM/TN), while HM classifications C and D are referred to as HM false-positive (HM/FP).

Table 2(a) summarizes the results of the classification analysis of the 58 HAL+ lesions observed with HM: 36 true-positive (HAL/TP) and 22 false-positive (HAL/FP). With the help of HM cystoscopy, 32/33 (97%) HAL/TP lesions with clinical *in situ* visualized vascularization could be confirmed, and 17/20 (85%) HAL/FP lesions with a visible vascularization could be rejected. The cancerous lesion that was not confirmed by our HM method (HAL/TP-HM/FN) was infiltrated by a sarcomatoid carcinoma. Conversely, the three lesions with vascular irregularities that were described as noncancerous by the histopathologist (HAL/FP-HM/FP) had the following histology: granulomatous inflammation, von Brunn nests that mimic urothelial carcinoma, and lymphoid infiltration, respectively.

Table 2(b) summarizes the results of the visual classification of the 45 flat HAL+ lesions observed with high magnification: 24 true-positive (HAL/TP) and 21 false-positive

(HAL/FP). With the help of HM cystoscopy, 22/22 (100%) HAL/TP flat lesions with visualized vascularization could be confirmed, and 17/19 (89.5%) HAL/FP lesions with a visible vascularization could be rejected.

4 Discussion

Over the last years, fluorescence cystoscopy has been established as the standard method for early bladder cancer detection in the European Union.^{14,27} Fluorescence cystoscopy is particularly useful at improving the detection of flat lesions, such as pTis and pTa.⁹ However, this technique has been related to a relatively high number of false-positive sites. Areas with a higher cellular turnover like metaplasia, hyperplasia, and residual inflammation also accumulate PpIX and, in that sense, fluoresce similarly to malignant tissue.¹⁴ Grimbergen et al. showed that several factors, including drug uptake and enzymatic activity, have been known to influence the production and conversion or depletion of PPIX after exogenous application of the ALA or ALA-esters.²⁸ Jichinski et al. speculated that false-positives can arise, in certain specific cases, from oblique illumination of the mucosa if the distal end of the endoscope is too close to the bladder wall.²⁹ Indeed, when the tissue is illuminated tangentially, it may produce a high level of fluorescence on the normal mucosa, particularly at the bladder neck and the trigone.³⁰ Additionally, bladder mucosa exposed to intravesical therapy in the weeks prior to fluorescence cystoscopy could also exhibit a higher rate of false-positive lesions.^{28,31} Draga et al. also showed that the false-positive rate decreases during the first 12 weeks after the latest resection.³²

In this study, we aimed to differentiate vascular patterns between nonmalignant, false-positive and malignant, true-positive changes in the bladder. Several groups have previously developed systems able to acquire images at the cellular level in the gastrointestinal tract,³³ even in the bladder,³⁴ but it appears that this approach has several limitations, particularly the microscopic field of view and the need for additional contrast dyes.³⁴ Scanning of the whole organ is thus not realistic in a clinical environment. Therefore, we have focused our research on the characterization of vascular patterns on suspicious sites already localized by Hexvix[®] fluorescence cystoscopy. In this configuration, a fluorescent site can easily be characterized with high magnification by turning the knob, adjusting the distance, and switching to the appropriate illumination light. This approach is very convenient since it allows visualization of the bladder using fluorescence and white light, both in the low- and the high-magnification regime, without changing the cystoscope.

Bladder cancer is often multifocal in nature. In this study, due the bladder ovoid geometry, this rigid cystoscope prototype with small viewing angle (25 deg) does not allow instrumental access to all parts of the bladder. In particular, the anterior wall and dome could not be imaged easily. Thus, in the statistics, the number of sites that are observed with the HM cystoscope is much smaller than the total number of fluorescence positive sites observed. We reviewed both flat and papillary fluorescence positive sites. In each papillary tumor, we have observed the so-called intrapapillary loops, where the capillaries appear like small rings of about 50 μm in diameter close to the surface. The shape of the vessels was in good

agreement with those observed in other organs.²²

All cystoscopy results can be more or less affected by the urologist learning curve. In particular, the rejection of false-positives highly depends on the physician's experience. The nonperfect specificity of the well-established drug Hexvix[®] has also been observed in larger HAL phase III studies.^{11,12} Our false-positive rate 68/178 (38%) is in fact in good agreement to what has been obtained in the latter (39%). In the present study, HAL cystoscopy detects 57% (107/68) more non-muscle-invasive lesions, including dysplasia, pTa, pT1, and pTis. Although there is an increase in the number of false-positive lesions, this clearly indicates a major advantage of HAL cystoscopy versus conventional WL cystoscopy, because it will allow a more complete resection.¹⁶

The three HM/FPs (see Table 2(a) and 2(b)) that are not cancerous lesions are tissues of identified types that may also induce modulation of the superficial vascularization that presumably supports cellular changes at the surface of the urothelium.³⁵ Conversely, no vascular alteration could be observed with our setup on the HM-FN lesion, even if it was protruding out of the bladder wall, probably because this pathology was not originated in the bladder mucosa.

Our results were based on the urologist-subjective appreciation, whereas an image analysis method for quantifying blood vessels could be helpful to aim at greater objectivity. Experiments on small blood vessels in the chorioallantoic membrane (CAM) model have led to the development of a multistep mathematical procedure to obtain a skeleton representation of the vessels and capillaries.³⁶ Similarly, software analysis of retinal vasculature images highlighted the potential of defining site-based parameters, such as local vessel diameter, fractal dimension, and tortuosity.³⁷ We are currently working at the integration of these quantification algorithms in our procedure. This may be of interest to assess the status of sites appearing positive during fluorescence cystoscopy. The next generation of prototypes with a better image quality may help algorithms to run with fewer artifacts.

Tables 2(a) and 2(b) illustrate that HM image acquisition may be impaired by missing some vascular patterns while looking at the fluorescence positive sites (5 for all lesions, 4 for flat lesions). Recent studies have targeted the hemoglobin absorption peaks using the narrow-band imaging technology.³⁸ At present, we are investigating the potential use of selected excitation wavelengths (data not shown) to improve the contrast between the vessels and the surrounding mucosa. This may help to point out the optimal vessels (depth and size) to discriminate FP from TP fluorescence positive sites. Furthermore, an increase in the cystoscope contact pressure may lead to a decrease in the superficial blood flow, and thus a decrease in reflectance light absorption, and hence the vessels close to the surface may disappear from the field of view. A spacer may be added to the cystoscope in the future to avoid this effect.

The observations made on exophytic lesions reveal a distinct pattern of vascularization, with loops sprouting along the papillary. In conjunction with a histochemical analysis of the biopsies, this approach may serve as a visual method for staging and grading of the exophytic bladder carcinomas.

The rigid cystoscope used in the present study prevents the visualization of the proximal part of the bladder wall and has evident drawbacks regarding bladder accessibility. However,

this cystoscope prototype helped us to demonstrate the proof-of-principle of this vessel characterization technique to identify false-positive lesions. This HM cystoscope approach can also be used for the characterization of sites suspicious under white light, or detected by other diagnostic techniques, including hypericin fluorescence cystoscopy.³⁹

In summary, we claim that this “detect-and-characterize” procedure based on a high-magnification cystoscope is very convenient since no change of endoscope is required to switch between the fluorescence detection and tissue vascular characterization modes. Therefore, with a rejection rate (97%) of FP lesions, HM is likely to be a noninvasive, simple, and convenient approach to reduce the number of biopsies and improve patient management.

Acknowledgments

This study was supported by Swiss National Science Foundation Grant No. 205320-116556/1. We would also like to thank Dr. Julia Jacobi for generous financial support. We thank the physicians at CHUV University Hospital for their contribution and advice (Drs. Valentin Praz, Cédric Treuthardt, Yves Chollet, Yassine Zarkik, Arnaud Doerfler, Laurent Vaucher, Thomas Tawadros, Cécile Tawadros, and Matieu Uffer).

References

- Z. Kirkali, T. Chan, M. Manoharan, F. Algaba, C. Busch, L. Cheng, L. Kiemeny, M. Kriegmair, R. Montironi, W. M. Murphy, I. A. Sesterhenn, M. Tachibana, and J. Weider, “Bladder cancer: epidemiology, staging and grading, and diagnosis,” *Urology* **66**(6 Suppl. 1), 4–34 (2005).
- W. Oosterlinck, A. V. Bono, D. Mack, R. Hall, R. Sylvester, C. De Balincourt, and M. Brausi, “Frequency of positive biopsies after visual disappearance of superficial bladder cancer marker lesions,” *Eur. Urol.* **40**(5), 515–517 (2001).
- M. J. Droller, “Biological considerations in the assessment of urothelial cancer: a retrospective,” *Urology* **66**(5 Suppl.), 66–75 (2005).
- D. Jocham, F. Witjes, S. Wagner, B. Zeylemaker, J. Van Moorselaar, M. O. Grimm, R. Muschter, G. Popken, F. König, R. Knüchel, and K. H. Kurth, “Improved detection and treatment of bladder cancer using hexaminolevulinate imaging: a prospective, phase III multicenter study,” *J. Urol.* **174**(3), 862–866 (2005).
- J. C. Kennedy, R. H. Pottier, and D. C. Pross, “Photodynamic therapy with endogenous protoporphyrin IX: basic principles and present clinical experience,” *J. Photochem. Photobiol., B* **6**(1–2), 143–148 (1990).
- J. C. Kennedy and R. H. Pottier, “Endogenous protoporphyrin IX, a clinically useful photosensitizer for photodynamic therapy,” *J. Photochem. Photobiol., B* **14**(4), 275–292 (1992).
- P. Uehlinger, M. Zellweger, G. Wagnieres, L. Juillerat-Jeanneret, H. van den Bergh, and N. Lange, “5-aminolevulinic acid and its derivatives: physical chemical properties and protoporphyrin IX formation in cultured cells,” *J. Photochem. Photobiol., B* **54**(1), 72–80 (2000).
- P. Jichlinski and D. Jacqmin, “Photodynamic diagnosis in non-muscle-invasive bladder cancer,” *Eur. Urol. Suppl.* **7**(7), 529–535 (2008).
- P. Jichlinski, H. J. Leisinger, L. Guillou, N. Lange, H. Van den Bergh, S. J. Karlsen, B. Brennhovd, P. U. Malmström, E. Johansson, D. Jocham, and T. Gärtner, “Hexyl aminolevulinate fluorescence cystoscopy: a new diagnostic tool for the photodiagnosis of superficial bladder cancer—a multicenter study,” *J. Urol.* **170**(1), 226–229 (2003).
- J. Schmidbauer, F. Witjes, N. Schmeller, R. Donat, M. Susani, and M. Marberger, “Improved detection of urothelial carcinoma *in situ* with hexaminolevulinate fluorescence cystoscopy,” *J. Urol.* **171**(1), 135–138 (2004).
- H. B. Grossman, L. Gomella, Y. Fradet, A. Morales, J. Presti, C. Ritenour, U. Nseyo, and M. J. Droller, “A phase III, multicenter comparison of hexaminolevulinate fluorescence cystoscopy and white light cystoscopy for the detection of superficial papillary lesions in patients with bladder cancer,” *J. Urol.* **178**(1), 62–67 (2007).
- Y. Fradet, H. B. Grossman, L. Gomella, S. Lerner, M. Cookson, D. Albala, M. J. Droller, and P. B. S. Group, “A comparison of hexaminolevulinate fluorescence cystoscopy and white light cystoscopy for the detection of carcinoma *in situ* in patients with bladder cancer: a phase III, multicenter study,” *J. Urol.* **178**(1), 68–73, discussion 73 (2007).
- D. I. Daniltchenko, C. R. Riedl, M. D. Sachs, F. Koenig, K. L. Daha, H. Pflueger, S. A. Loening, and D. Schnorr, “Long-term benefit of 5-aminolevulinic acid fluorescence assisted transurethral resection of superficial bladder cancer: 5-year results of a prospective randomized study,” *J. Urol.* **174**(6), 2129–2133, discussion 2133 (2005).
- J. A. Witjes and J. Douglass, “The role of hexaminolevulinate fluorescence cystoscopy in bladder cancer,” *Nat. Clin. Pract. Urol.* **4**(10), 542–549 (2007).
- S. Denzinger, M. Burger, B. Walter, R. Knuechel, W. Roessler, W. F. Wieland, and T. Filbeck, “Clinically relevant reduction in risk of recurrence of superficial bladder cancer using 5-aminolevulinic acid-induced fluorescence diagnosis: 8-year results of prospective randomized study,” *Urology* **69**(4), 675–679 (2007).
- M. Babjuk, V. Soukup, R. Petrik, M. Jirsa, and J. Dvoracek, “5-aminolaevulinic acid-induced fluorescence cystoscopy during transurethral resection reduces the risk of recurrence in stage Ta/T1 bladder cancer,” *BJU Int.* **96**(6), 798–802 (2005).
- A. P. M. van Der Meijden, R. Sylvester, W. Oosterlinck, E. Solsona, A. Boehle, B. Lobel, and E. Rintala, “EAU guidelines on the diagnosis and treatment of urothelial carcinoma *in situ*,” *Eur. Urol.* **48**(3), 363–371 (2005).
- P. J. S. Charlesworth and A. L. Harris, “Mechanisms of disease: angiogenesis in urologic malignancies,” *Nat. Clin. Pract. Urol.* **3**(3), 157–169 (2006).
- F. Reiber, O. Ozer, M. Pins, B. D. Jovanovic, S. Eggener, and S. C. Campbell, “p53 and microvessel density in primary resection specimens of superficial bladder cancer,” *J. Urol.* **167**(3), 1469–1474 (2002).
- J. E. East, N. Suzuki, P. Bassett, M. Stavrindis, H. J. Thomas, T. Guenther, P. P. Tekkis, and B. P. Saunders, “Narrow band imaging with magnification for the characterization of small and diminutive colonic polyps: pit pattern and vascular pattern intensity,” *Endoscopy* **40**(10), 811–817 (2008).
- Y. Kumagai, M. Iida, and S. Yamazaki, “Magnifying endoscopic observation of the upper gastrointestinal tract,” *Digest. Endosc.* **18**(3), 165–172 (2006).
- K. Shibuya, H. Hoshino, M. Chiyo, A. Iyoda, S. Yoshida, Y. Sekine, T. Iizasa, Y. Saitoh, M. Baba, K. Hiroshima, H. Ohwada, and T. Fujisawa, “High magnification bronchovideoscopy combined with narrow band imaging could detect capillary loops of angiogenic squamous dysplasia in heavy smokers at high risk for lung cancer,” *Thorax* **58**(11), 989–995 (2003).
- K. Shibuya, H. Hoshino, M. Chiyo, K. Yasufuku, T. Iizasa, Y. Saitoh, M. Baba, K. Hiroshima, H. Ohwada, and T. Fujisawa, “Subepithelial vascular patterns in bronchial dysplasias using a high magnification bronchovideoscope,” *Thorax* **57**(10), 902–907 (2002).
- H. Inoue, T. Honda, K. Nagai, T. Kawano, K. Yoshino, K. Takeshita, and M. Endo, “Ultra-high magnification endoscopic observation of carcinoma *in situ* of the esophagus,” *Digest. Endosc.* **9**(1), 16–18 (1997).
- F. K. Mostofi, L. H. Sobin, and H. Torloni, “Histological typing of urinary bladder tumors,” International Histological Classification of Tumors, No. 10, WHO, Geneva (1973).
- J. I. Epstein, M. B. Amin, V. R. Reuter, F. K. Mostofi, F. Algaba, W. C. Allsbrook, A. G. Ayala, M. J. Becich, A. L. Beltran, L. Boccon-Gibod, D. G. Bostwick, C. Busch, C. J. Davis, J. N. Eble, C. S. Foster, M. Furusato, D. J. Grignon, P. A. Humphrey, E. A. Ishak, S. L. Johansson, E. C. Jones, L. G. Koss, H. S. Levin, W. M. Murphy, R. O. Petersen, A. Renshaw, J. Y. Ro, J. R. Ross, I. A. Sesterhenn, J. R. Strigley, S. Suzigan, J. B. Tomaszewski, P. Troncoco, L. D. True, M. A. Weiss, T. M. Wheeler, and R. H. Young, “The World Health Organization/International Society of Urological Pathology consensus classification of urothelial (transitional cell) neoplasms of the urinary bladder,” *Am. J. Surg. Pathol.* **22**(12), 1435–1448 (1998).
- M. C. Hall, S. S. Chang, G. Dalbagni, R. S. Pruthi, J. D. Seigne, E. C. Skinner, J. S. Wolf Jr., and P. F. Schellhammer, “Guideline for the management of nonmuscle-invasive bladder cancer (stages Ta, T1, and Tis): 2007 update,” *J. Urol.* **178**(6), 2314–2330 (2007).

28. M. C. Grimbergen, C. F. van Swol, T. G. Jonges, T. A. Boon, and R. J. van Moorselaar, "Reduced specificity of 5-ALA induced fluorescence in photodynamic diagnosis of transitional cell carcinoma after previous intravesical therapy," *Eur. Urol.* **44**(1), 51–56 (2003).
29. P. Jichlinski, M. Forrer, J. Mizeret, T. Glanzmann, D. Braichotte, G. Wagnières, G. Zimmer, L. Guillou, F. Schmidlin, P. Graber, H. D. Van Bergh, and H. J. Leisinger, "Clinical evaluation of a method for detecting superficial transitional cell carcinoma of the bladder by light-induced fluorescence of protoporphyrin IX following topical application of 5-aminolevulinic acid: preliminary results," *Lasers Surg. Med.* **20**(4), 402–408 (1997).
30. D. Zaak, W. F. Wieland, C. G. Stief, and M. Burger, "Routine use of photodynamic diagnosis of bladder cancer: practical and economic issues," *Eur. Urol. Suppl.* **7**(7), 536–541 (2008).
31. R. O. Draga, M. C. Grimbergen, E. T. Kok, T. N. Jonges, C. F. van Swol, and J. L. Bosch, "Photodynamic diagnosis (5-aminolevulinic acid) of transitional cell carcinoma after bacillus calmette-guerin immunotherapy and mitomycin c intravesical therapy," *Eur. Urol.* **57**(4), 655–660 (2010).
32. R. O. Draga, M. C. Grimbergen, E. T. Kok, T. N. Jonges, and J. L. Bosch, "Predictors of false positives in 5-aminolevulinic acid-induced photodynamic diagnosis of bladder carcinoma: identification of patient groups that may benefit most from highly specific optical diagnostics," *Urology* **74**(4), 851–856 (2009).
33. T. D. Wang, S. Friedland, P. Sahbaie, R. Soetikno, P. L. Hsiung, J. T. Liu, J. M. Crawford, and C. H. Contag, "Functional imaging of colonic mucosa with a fibered confocal microscope for real-time *in vivo* pathology [see comment]," *Clin. Gastroenterol. Hepatol.* **5**(11), 1300–1305 (2007).
34. G. A. Sonn, S. N. Jones, T. V. Tarin, C. B. Du, K. E. Mach, K. C. Jensen, and J. C. Liao, "Optical biopsy of human bladder neoplasia with *in vivo* confocal laser endomicroscopy," *J. Urol.* **182**(4), 1299–1305 (2009).
35. A. Romanenko, K. Morimura, H. Wanibuchi, M. Wei, W. Zaporin, W. Vinnichenko, A. Kinoshita, A. Vozianov, and S. Fukushima, "Urinary bladder lesions induced by persistent chronic low-dose ionizing radiation," *Cancer Sci.* **94**(4), 328–333 (2003).
36. P. Nowak-Sliwiska, J.-P. Ballini, G. Wagnières, and H. van den Bergh, "Processing of fluorescence angiograms for the quantification of vascular effects induced by anti-angiogenic agents in the CAM model," *Microvasc. Res.* **79**(1), 21–28 (2010).
37. M. B. Vickerman, P. A. Keith, T. L. McKay, D. J. Gedeon, M. Watanabe, M. Montano, G. Karunamuni, P. K. Kaiser, J. E. Sears, Q. Ebrahem, D. Ribita, A. G. Hylton, and P. Parsons-Wingerter, "VES-GEN 2D: automated, user-interactive software for quantification and mapping of angiogenic and lymphangiogenic trees and networks," *Anat. Rec.* **292**(3), 320–332 (2009).
38. H. W. Herr and S. M. Donat, "A comparison of white-light cystoscopy and narrow-band imaging cystoscopy to detect bladder tumour recurrences," *BJU Int.* **102**(9), 1111–1114 (2008).
39. R. Bhuvaneshwari, P. S. Thong, Y. Y. Gan, K. Soo, and M. Olivo, "Evaluation of hypericin-mediated photodynamic therapy in combination with angiogenesis inhibitor bevacizumab using *in vivo* fluorescence confocal endomicroscopy," *J. Biomed. Opt.* **15**(1), 011114 (2010).